

ON THE MECHANISM OF FORWARD EMITTED  
FRAGMENT PRODUCTION IN  $^{22}\text{Ne} + ^9\text{Be}$  REACTION  
IN THE VICINITY OF THE FERMI ENERGY

A.G. ARTUKH<sup>a</sup>, A. BUDZANOWSKI<sup>b</sup>, G. KAMIŃSKI<sup>a,b</sup>, W. KANTOR<sup>b</sup>  
S.A. KLYGIN<sup>a</sup>, E. KOZIK<sup>b†</sup>, YU.M. SEREDA<sup>a,c</sup>, J. SZMIDER<sup>b</sup>  
YU.G. TETEREV<sup>a</sup>, A.N. VORONTZOW<sup>a,c</sup>

<sup>a</sup>Joint Institute for Nuclear Researches, 141980 Dubna, Russia

<sup>b</sup>The H. Niewodniczański Institute of Nuclear Physics PAN  
Radzikowskiego 152, 31-342 Kraków, Poland

<sup>c</sup>Institute for Nuclear Research  
Prospekt Nauki 47, 252650 Kiev-22, Ukraine

*(Received May 19, 2008; revised version received November 17, 2008)*

The charge and relative velocity distributions of forward emitted fragments in the  $^{22}\text{Ne} + ^9\text{Be}$  reaction at bombarding energy of 40 AMeV are presented. Experimental results are compared with the quantum molecular dynamics (QMD) model taking into account in calculations the mean field-like effects and the two-body scattering term. In the theoretical analysis a subsequent statistical decay of excited primary reaction products following the QMD predictions is applied. The assumption of two scenarios responsible for production of forward emitted fragments results in a good representation of the data suggesting a preferential contribution of the mean field-like effects in production mechanism.

PACS numbers: 25.70.-z, 24.10.Cn

## 1. Introduction

Heavy ion reactions at intermediate energies, especially in the Fermi energy vicinity, are of considerable interest for studying the transitional phenomena characteristic for this energy domain [1–4]. This domain has to be seen as a region for which the high energy concepts (nucleon–nucleon collisions) are downward extended and low energy ideas (a mean field approximation) are upward expanded. At energies less than 10–15 AMeV for

---

<sup>†</sup> Ewa.Kozik@ifj.edu.pl

central collisions the complete fusion, corresponding to the total momentum transfer, is observed. The peripheral and semi-peripheral collisions are characterized by the presence of final fragments resulting from binary quasi elastic and deep inelastic reactions, nuclei pass through each other keeping a strong memory of their initial attributes. At bombarding energies above  $\sim 30$  AMeV the reaction mechanism would change drastically, the processes familiar from below  $\sim 10$  AMeV would disappear and new mechanisms would appear with rising importance according to the increment of incoming energy. Fusion in the sense of complete amalgamation of the colliding nuclei has been found to fade away as a consequence of the increasing inefficiency of the mean field to damp the relative motion of two reaction partners. For intermediate energies a mean field approximation results in system transparency, on the other hand the inclusion of two-body collisions supports a creation of composite system (faster relaxation, reduction of nucleus temperature, equilibration of configuration and momentum space due to non equilibrium emission of nucleons and clusters). Moreover, in the case of collision velocities close to or exceeding the Fermi velocity a nucleus no longer reacts as a whole to each change resulting from the interaction. A portion of nucleus mass may be removed from a nucleus or local heating or compression of a part of the nucleus may occur. Concluding, in a description of heavy ion collisions at intermediate energy, mean field effects, known to be dominant below 10 AMeV, have to be supplemented by nucleon–nucleon collisions, which prevail at higher energies. For the theoretical study of  $^{22}\text{Ne}(40 \text{ AMeV})+^9\text{Be}$  reaction the CHIMERA code [5], the numerical realization of quantum molecular dynamics [6, 7], has been used. The model belongs to the class of models [8–11] which links low [12–14] and high energy [15–18] regimes, where the known reaction mechanisms are completely different. The aim of our work is to recognize the contributions of mechanisms corresponding to low and high energy domain in creation of the forward emitted fragments in  $^{22}\text{Ne} + ^9\text{Be}$  reaction in the vicinity of the Fermi energy.

The paper is organized as follows: Section 2 presents briefly the experimental set up, the short description of the model is outlined and the model applicability in description and interpretation of the experimental data is examined. The summary and conclusions are presented in Section 3.

## 2. Analysis

### 2.1. Experimental set up

The experiment was performed using 40 AMeV  $^{22}\text{Ne}$  beam from the U-400M cyclotron installed at the Flerov Laboratory of Nuclear Reactions, JINR Dubna. The beam was focused on the 14 mg/cm<sup>2</sup> Be target placed at the entrance of the double achromatic fragment separator COMBAS op-

erating in the spectrometry regime. Forward emitted ( $\theta_{\text{lab}} \leq 2.5^\circ$ ) products from the  $^{22}\text{Ne}$  (40 AMeV) +  $^9\text{Be}$  reaction were separated, mass and charge identified ( $3 \leq Z \leq 12$ ,  $6 \leq A \leq 25$ ), and detected by the combination of the magnetic rigidity and  $\Delta E - E$  ( $\Delta E = 0.38$  mm, 3.5 mm,  $E = 7.5$  mm silicon detectors) methods. The details of experimental set-up and procedure are presented in Refs. [19, 20].

## 2.2. Description of the applied model

The code CHIMERA (Code for Heavy Ion Medium Energy ReAction) [5] being the numerical realization of the quantum molecular dynamics (QMD) approach [6] has been used in the study of the  $^{22}\text{Ne}(40 \text{ AMeV}) + ^9\text{Be}$  reaction. In the QMD approach nucleons, each represented by Gaussians with non-zero width in phase-space, evolve according to classical Hamilton equations of motion under the force field generated by the sum of all the nucleon–nucleon interactions ( $N$ -body dynamics). The interactions used in this realization of QMD are approximated by the two- and three-body effective Skyrme interaction supplemented by the Coulomb potential and the momentum dependent Pauli potential. Pauli potential plays an important role during initialization of a cold nucleus preventing the existence of the nucleons of the same kind too close in the phase-space. The mean field-like dynamics is supplemented by the two-body collisions (hard scattering) in the spirit of cascade calculations developed successfully for description of relativistic heavy ion reactions. Monte Carlo procedure simulates the influence of the scattering term on the time evolution of the system. If the spatial distance of two nucleons is less than the distance determined by the free nucleon–nucleon cross-section they become candidates for scattering [4]. The energy-dependent free nucleon–nucleon cross-section is taken according to Ref. [7], however, due to the Pauli blocking, the effective cross-section is smaller. As a consequence of collision two particles can scatter elastically, inelastic collisions are not taken into account. After dynamical evolution a cluster search routine is applied. Each fragment is recognized using a minimum distance chain procedure. Then mass number, atomic number, position, linear momentum, binding and excitation energy, spin of fragment are calculated. At the end of the dynamical stage of the reaction the statistical decay model is applied to make possible a comparison of experimental data with theoretical predictions.

## 2.3. Results and discussion

### 2.3.1. Charge distribution

CHIMERA calculations were performed using the hard and soft equation of state (EoS). Dynamic calculations performed on an event-by-event basis were stopped at  $t = 600$  fm/ $c$ . The number of considered events was

50 000 and the simulations were done in the full range of impact parameter ( $b = 0 \div 6$  fm,  $bdb$  weighted distribution). Taking into account that at the end of the dynamical stage of the reaction the CHIMERA code produces fragments not only in their ground states, the simulations were supplemented by the statistical decay process. In the frame of the model the amount of excitation energy and spin deposited in the fragments is determined, so the application of the statistical decay model is possible. The code GEMINI [21] using the Monte Carlo technique follows the decay chains of hot nuclei considering all possible binary partition from light particle emission to symmetric division. The simulation of the statistical decay process proceeds until the final nucleus excitation energy forbids the further evaporation and no more particles can be emitted.

In Fig. 1 the hybrid model (CHIMERA+GEMINI) predicted charge distribution of final cold products emitted at forward angles in comparison with experimental results are presented. The yield of  $^{22}\text{Ne}$  products is excluded from the analysis due to difficulties of the experimental separation the projectile and the ejectile. The studied results of simulations under hard EoS assumption were extended to fragments appearing at  $\theta_{\text{lab}} \leq 5^\circ$  to obtain a sufficient statistics of model predictions for comparison with experimental data. A close investigation of the sensitivity of the model predictions on the particular choice of the angular range taken into account showed a weak dependence for the ranges  $\theta_{\text{lab}} \leq 3^\circ$ ,  $\theta_{\text{lab}} \leq 5^\circ$ ,  $2^\circ \leq \theta_{\text{lab}} \leq 7^\circ$ . The findings that the broadening of angle interval or the shift of limits of interval does not change the general character of model distributions and, as a consequence, does not influence on the final remarks, may be drawn. As is shown in Fig. 1 the normalization procedure realized by satisfactory conformity of the model (dashed line) and measured (dots) distributions for

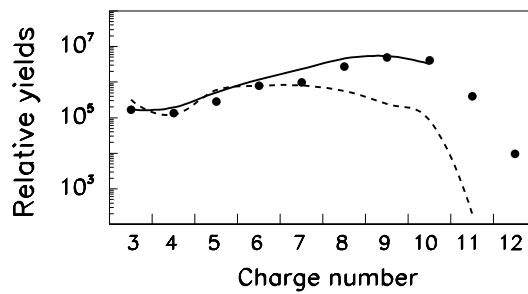


Fig. 1. The charge distribution of forward emitted fragments in the  $^{22}\text{Ne}(40 \text{ AMeV}) + ^9\text{Be}$  reaction. The dashed line represents results of CHIMERA+GEMINI calculations performed with collision term, the solid curve corresponds to the model results with suppression of collisions, the symbols represent the experimental data.

$Z_{\text{frag}} \leq 7$  results in complete disagreement for  $Z_{\text{frag}} > 7$ . Similar results, unable to properly describe the shape of experimentally obtained charge distribution, were obtained in the case of soft EoS calculations. In the face of complete defeat of applied procedure the calculation was repeated assuming the exclusion of two-body collisions (only the mean field-like effects are taken into account in phase-space time evolution in QMD approach). As is presented in Fig. 1. the exclusion of collision term from calculations assuming the hard EoS, leads to satisfactory agreement of the model results (solid line) with experimentally obtained charge distribution (dots). It must be pointed out that the agreement is attained only for  $Z_{\text{frag}} \leq Z_{\text{proj}}$ . The mean field-like effects are not strong enough to hold the system together and to form the composite system, hence the complete/incomplete fusion is not achieved resulting in the absence of fragments with  $Z > Z_{\text{proj}}$ . The inclusion of collision term in QMD calculations produces the fragments with  $Z = 11, 12, 13$  although due to the efficiency of nucleon–nucleon collisions in conversion the energy into the heat these fragments are excited and undergo a statistical decay. Primary fragments with  $Z = 12, 13$  do not survive, feeding the lower region of  $Z$ -distribution, cold products with  $Z = 11$  occur finally in the charge distribution although the theoretical yield is considerably reduced in relation to the experimental one.

Concluding, the choice of applied EoS type (hard/soft) does not influence on the shape of charge distribution in the case when the mean field-like effects and the collision term is taken into account in simulations. It points to the prevailing role of two-body effects in construction of the final nucleon phase-space, the form of the interaction potentials is of a second rank. On the other hand, the mean field-like effects without collision term produce completely different charge distributions under assumption of the hard and soft EoS. The choice of hard EoS and the mean field-like effects alone reproduces the experimental charge distribution in the region of  $Z_{\text{frag}} \leq Z_{\text{proj}}$  rather well. So, in the first approximation in preliminary analysis we may conclude carefully that the forward emitted fragments with  $Z \leq 10$  in the  $^{22}\text{Ne}(40 \text{ AMeV}) + ^9\text{Be}$  reaction are produced at most by the mechanism adequate to the low energy regime where two-body collisions are forbidden.

### 2.3.2. Velocity spectra

In the experiment the velocities of isotopes of fragments with  $Z = 3 \div 10$  emitted at forward angles were measured. According to the considerations presented in the previous section the experimentally obtained relative velocity spectra of strongest abundant isotopes have been compared with model predictions under assumptions of hard EoS and absence of the collision term. The bottom and upper limits of the experimentally obtained spectra of relative velocities,  $v_{\text{rel}}$ , were 0.55 and 1.3, respectively, although the ranges

of distributions are correlated with  $Z_{\text{frag}}$ . With increasing fragment charge number the increment of lower limit of  $v_{\text{rel}}$  is observed. The character of experimental spectra is also dependent on fragment charge number, for lightest nuclei the distributions are roughly flat in the full range, while with increase of  $Z$  the bump spread in the vicinity of velocity corresponding to projectile velocity grows in strength. The model predicted distributions are tightened significantly in relation to the experimentally obtained results reaching the bottom limit at the value of 0.7, 0.8, depending on considered isotope, however the positions of experimentally obtained maxima of the distributions are followed roughly by theoretical ones. It is a consequence of switching off the collision term, the inefficiency of the mean field-like effects to dump the relative motion of two reaction partners is manifested in the bottom limit of calculated  $v_{\text{rel}}$  value. The nucleon–nucleon scattering may cause a stronger phase-space rearrangement resulting in a variation of initial physical features [7, 9, 22]. The inclusion of the two-body term in QMD calculations is expected to change the fragment velocity in relation to projectile velocity. The model velocity distributions obtained from calculations taking into account the mean field-like and the scattering term are characterized by a significant shift of the maximum positions and a shift of the distribution limits toward lower values in relation to the results obtained from the mean field-like effects calculations. The results of simulations performed under assumption of inclusion and exclusion of the collision term allowed to obtain a satisfactory description of high and low part of velocity spectra, respectively. It must be pointed out that for the correct description of the experimental velocity spectra by the model predictions the contributions corresponding to the mean field-like processes and the mean field-like processes

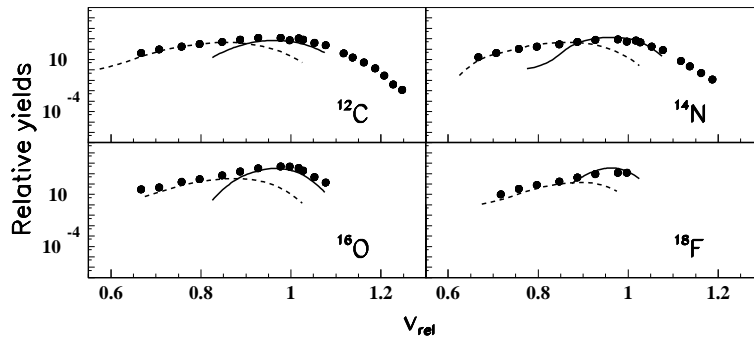


Fig. 2. Relative velocity distributions of  $^{12}\text{C}$ ,  $^{14}\text{N}$ ,  $^{16}\text{O}$  and  $^{18}\text{F}$ . The dashed and solid lines represent the model calculations performed under assumption of inclusion and exclusion of collision term, respectively. Experimental data are represented by symbols.

supplemented by the collision term are not equally weighted. The relative contributions were determined by comparison of model predicted and measured velocity spectra for  $^{12}\text{C}$ ,  $^{14}\text{N}$ ,  $^{16}\text{O}$ ,  $^{18}\text{F}$  (the most abundant isotopes with charge number not far from the projectile charge). The contribution of dissipative part occurred to be significantly suppressed (by a factor equal to 0.23) respecting the non-dissipative, high velocity part. As is seen in Fig. 2 an idea of two kinds of mechanisms responsible for production of forward emitted fragments results in a well description of measured velocity spectra by model predictions. Obtained in this way the values of scaling factors were used for construction of velocity distribution for all isotopes under consideration. The results of analysis are presented in Figs. 3, 4.

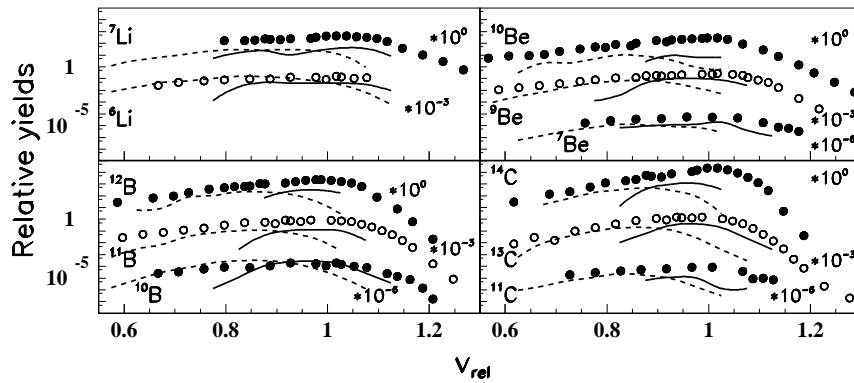


Fig. 3. Relative velocity distributions of fragments with  $Z = 3-6$  resulting from CHIMERA+GEMINI calculations. Panels present the distributions for Li, Be, B, C isotopes. Symbols represent the experimental data, results of calculations with and without collision term are represented by the dashed and solid curve, respectively. Multiplication factors have been used to clarify the figures.

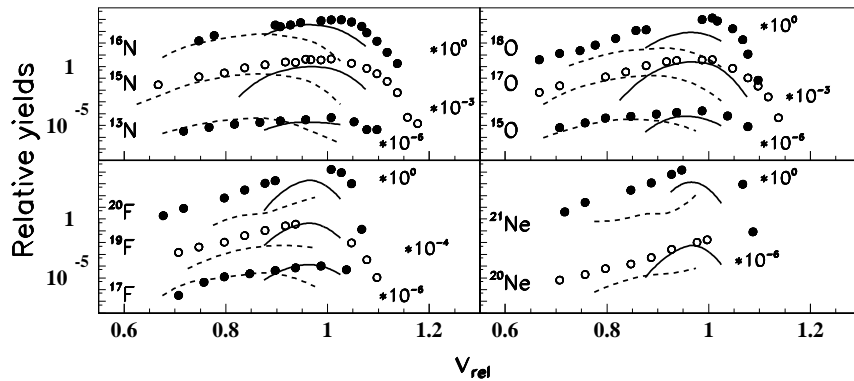


Fig. 4. Same as Fig. 3 for fragments with  $Z = 7-10$  (N, O, F, Ne).

The description turns out rather well, although we may state that:

- for light fragments with  $A = 2Z$  (Li, B) the model description of experimental data occurs to be of the similar quality as for heavier fragments,
- using the factors determined for most abundant C, N, O, F isotopes, for  ${}^7\text{Li}$ ,  ${}^{10}\text{Be}$ ,  ${}^{18}\text{O}$ ,  ${}^{20}\text{F}$ ,  ${}^{21}\text{Ne}$  the velocity distributions are underestimated, indicating on the inadequate model predictions of neutron rich isotope production. The shapes of calculated spectra follow the experimental results manifesting the same strengths of respective reaction scenarios as obtained for isotopes with  $A = 2Z$ ,
- for  ${}^{19}\text{F}$ ,  ${}^{20}\text{Ne}$  the low velocity contribution corresponding to the mean field-like and collision term calculations obtained on the ground of the fitting procedure described above occurs to be insufficient. On the other hand in the case of  ${}^{11}\text{C}$ ,  ${}^{14}\text{C}$ ,  ${}^{15}\text{N}$ ,  ${}^{16}\text{N}$  the shapes of measured velocity spectra indicate on the stronger than predicted role of pure mean field-like effects in production of these fragments,
- the model is unable to describe the part of measured velocity spectra in the range exceeding the projectile velocity ( $v_{\text{rel}} > 1.05, 1.1$ ).

In the face of the correctness of the concept of two separate reaction scenarios responsible for the production of forward emitted fragments manifested in satisfactory model description of velocity spectra we have considered how this idea operates in the description of charge distribution. Because of  $\sim 20\%$  contribution of one- and two-body effects and  $\sim 80\%$  mean field-like contribution the modification of charge distribution obtained under assumption of pure mean field-like effects, reproducing the experimental data rather well, is expected to be of no great importance. So, the comparison of model results with experimental relative velocity distributions indicates that at least two scenarios of reaction are responsible for production of forward emitted fragments in  ${}^{22}\text{Ne}(40 \text{ AMeV}) + {}^9\text{Be}$  collisions. Calculations performed under assumption of absence of the scattering term, adequate for low energy regime, describe satisfactory measured charge distributions, on the other hand the simulations are unable to give a proper reproduction of the velocity spectra. To generate the velocities significantly reduced in respect of the projectile velocity the assumption of the other additional reaction picture is indispensable. The introduction of two-body effects involves that (i) the strength of the mean field effects is reduced by the collision term playing an essential role, (ii) in each nucleon–nucleon collision due to its random character the memory of the system is gradually lost resulting among other in energy damping. The low velocity tail is an indication of this energy dissipation. By comparison of experimental and theoretical velocity spectra

the contribution from one- and two-body picture has been estimated to be about four times weaker than the part corresponding to mean field-like scenario. Although it was found that there are isotopes ( $^{19}\text{F}$ ,  $^{20}\text{Ne}$ ), for which the proper description of the data requires the significant intensification of one- and two-body contribution in relation to the mean field-like part.

Our remarks concerning the leading role of the mean field-like effects are justified by the results obtained in the study of the forward emitted fragments in  $^{18}\text{O}(35 \text{ AMeV}) + ^9\text{Be}(^{181}\text{Ta})$  reactions [23]. Although the QMD approach taking into account mean field-like + two-body effects has predicted the charge distributions of fragments rather well, the comparison of theoretically and experimentally obtained velocity spectra demonstrates that the calculation procedure was not able to generate a proper description of velocity distributions. The high velocity part observed in experimental data for all analyzed fragments, not predicted by the model calculations, indicates the significant contribution of pure one-body mechanism in forward emitted fragment production.

### 3. Summary and conclusions

A hybrid model based on quantum molecular dynamics and statistical decay procedure was used for description of experimentally obtained charge and isotopic velocity distributions of forward emitted fragments in  $^{22}\text{Ne}(40 \text{ AMeV}) + ^9\text{Be}$  reaction. In the intermediate energy domain defined by bombarding energies between 15 and 100 MeV per nucleon the processes observed at low energies, dominated by mean field considerations, and at high energy reactions, for which nucleon–nucleon collisions play an important role, are expected. We found that the essential concept of quantum molecular dynamics model taking into account as well the mean field-like effects as the nucleon–nucleon collision term fails in reproduction of our data. The model is not able to describe properly the fragment charge and isotope relative velocity distributions. The results of calculations contribute only to the low part of velocity distributions. It illustrates the strong role played by the scattering term; even a relatively small number of collisions is enough to diminish significantly the fragment velocity. Our remarks meet the previous observations obtained for  $^{18}\text{O}(35 \text{ AMeV}) + ^9\text{Be}(^{181}\text{Ta})$  reactions [23]. The model reproduces the experimental charge distribution for  $^{22}\text{Ne}(40 \text{ AMeV}) + ^9\text{Be}$  reaction rather well when the artificial exclusion of the collision term is applied. Because the results of calculations using mean field models and quantum molecular dynamics model with blocked nucleon–nucleon collisions were found to be very similar [6, 24], it is expected that this form of QMD mimics the mean field approaches. Results of model simulations performed under assumption of collision term exclusion reproduce

quite well the high velocity part of  $v_{\text{rel}}$  distribution. On the other hand, the velocities corresponding to the dissipative processes are not predicted by the model calculations. The conclusion that can be drawn is that two scenarios responsible for production of measured fragments have to be taken into account. The comparison of model predictions with experimental data indicates that the forward emitted fragments are produced in a way characteristic to low energy regime (pure mean field-like effects) as well as in one- and two-body processes corresponding to intermediate energy domain. The analysis allows to draw the conclusions about the leading role of the mean field-like effects in production of forward emitted fragments. The application of the model shows that the charge and velocity distributions can be reasonably well reproduced by the model simulations taking into account about 80% and 20% contributions of pure one-body and mean field-like + two-body term scenarios, respectively. The fragment velocities exceeding meaningfully the projectile velocity are not predicted by the model calculations. Typical quasi-elastic processes for low energy regime like a direct cluster transfer may remove from the projectile nucleus nucleons with intrinsic Fermi velocity antialigned to the beam direction, leaving the final fragment in the state characterized by a velocity exceeding the projectile velocity. QMD approach treats the nuclear object like a set of individual nucleons which positions and linear momenta propagate according to classical equation of motion under the influence of the field created by the others nucleons optionally interacting via two-body effects. For the mean field-like as well as for mean field-like plus collision term treatments the excitation energy of recognized cluster obtained in the QMD calculations is high enough for the statistical evaporation of nucleon(s) calculated by means of GEMINI code. It seems that QMD simulations generally predict too high excitation energies of the primary fragments, regardless of the mean field-like or mean field-like plus collision term methods applied in calculations. So, the processes of direct removal of a few nucleons, treated as a complex system, leaving the final objects nearly cold, are beyond the limits of QMD approach.

## REFERENCES

- [1] H. Fuchs, K. Möring, *Rep. Prog. Phys.* **57**, 231 (1994).
- [2] E. Suraud, C. Grégoire, B. Tamain, *Prog. Part. Nucl. Phys.* **23**, 357 (1989).
- [3] B. Bordiere, M.F. Rivet, L. Tassan-Got, Internal Report IPNO-DRE-90-06.
- [4] G.F. Bertsch, S. Das Gupta, *Phys. Rep.* **160**, 189 (1988).
- [5] J. Łukasik, Z. Majka, *Acta Phys. Pol. B* **24**, 1959 (1993).
- [6] J. Aichelin, G. Peilert, A. Bohnet, A. Rosenhauer, H. Stöcker, W. Greiner, *Phys. Rev.* **C37**, 2451 (1988).

- [7] J. Aichelin, *Phys. Rep.* **202**, 233 (1991).
- [8] K. Niita, S. Chiba, T. Maruyama, T. Maruyama, H. Takada, T. Fukahori, Y. Nakahara, A. Iwamoto, *Phys. Rev.* **C52**, 2620 (1995).
- [9] S.R. Souza, L. de Paula, S. Leray, J. Nemeth, C. Ngô, H. Ngô, *Nucl. Phys.* **A571**, 159 (1994).
- [10] J. Aichelin, G. Bertsch, *Phys. Rev.* **C31**, 1730 (1985).
- [11] S.A. Bass, M. Belkacem *et al.*, *Prog. Part. Nucl. Phys.* **41**, 225 (1998).
- [12] P. Bonche, S.E. Koonin, J.W. Negele, *Phys. Rev.* **C13**, 1226 (1976).
- [13] S.E. Koonin, K.T.R. Davies, V. Maruhn-Rezwani, H. Feldmeier, S.J. Krieger, J.W. Negele, *Phys. Rev.* **C15**, 1359 (1977).
- [14] K.T.R. Davies, S.E. Koonin, *Phys. Rev.* **C23**, 20042 (1981).
- [15] J. Cugnon, *Phys. Rev.* **C22**, 1885 (1980).
- [16] J. Cugnon, T. Mizutani, J. Vandermuelen, *Nucl. Phys.* **A352**, 505 (1981).
- [17] J. Cugnon, *Nucl. Phys.* **A387**, 191c (1982).
- [18] Y. Yariv, Z. Fraenkel, *Phys. Rev.* **C20**, 227 (1979).
- [19] A.G. Artukh, G.F. Gridnev *et al.*, *Nucl. Instrum. Methods* **A426**, 605 (1999).
- [20] A.G. Artukh, G.F. Gridnev, M. Gruszecki, F. Kościelniak, A.G. Semchenkov, O.V. Semchenkova, Yu.M. Sereda, J. Szmider, Yu.G. Teterev, *Phys. Atom. Nucl.* **65**, 393 (2002).
- [21] R.J. Charity, M.A. McMahan, G.J. Wozniak, R.J. McDonald, L.G. Moretto, D.G. Saratites, L.G. Sobotka, G. Guarino, A. Pantaleo, L. Fiore, A. Gobbi, K.D. Hildenbrand, *Nucl. Phys.* **A483**, 371 (1988).
- [22] H. Kruse, B.V. Jacak, J.J. Molitoris, G.D. Westfall, H. Stöcker, *Phys. Rev.* **C31**, 1770 (1985).
- [23] A.G. Artukh, A. Budzanowski, G. Kamiński, W. Kantor, S.A. Klygin, E. Kozik, O.V. Semchenkova, Yu.M. Sereda, J. Szmider, Yu.G. Teterev, A.N. Vorontzow, *Acta Phys. Pol. B* **37**, 1875 (2006).
- [24] J. Aichelin, C. Hartnack, A. Bohnet, L. Zhuxia, G. Peilert, H. Stöcker, W. Greiner, *Phys. Lett.* **B224**, 34 (1989).